Food Chemistry 354 (2021) 129511

Contents lists available at ScienceDirect

Food Chemistry

journal homepage: www.elsevier.com/locate/foodchem

Detection of organophosphorus pesticides by nanogold/mercaptomethamidophos multi-residue electrochemical biosensor

Guozheng Zhao [a,*], Binhua Zhou [b], Xiuwen Wang [b], Jian Shen [b], Bo Zhao [b,*]

[a] Key Laboratory of Magnetic Molecules & Magnetic Information Materials Ministry of Education, The School of Chemistry and Material Science, College of Food Science, Shanxi Normal University, Linfen 041004, China
[b] National and Local Joint Engineering Research Center of Biomedical Functional Materials, School of Chemistry and Materials Science, Nanjing Normal University, Nanjing 210023, China

ARTICLE INFO

Keywords:
Detection
OPPs
Nanogold
Electrochemical biosensor
Acetylcholinesterase

ABSTRACT

Based on the successful synthesis of mercaptomethamidophos as a substrate, a novel nanogold/mercaptomethamidophos multi-residue electrochemical biosensor was designed and fabricated by combining nanoscale effect, strong Au–S bonds as well as interaction between acetylcholinesterase (AChE) and mercaptomethamidophos, which can simultaneously detect 11 kinds of organophosphorus pesticides (OPPs) and total amount of OPPs using indirect competitive method. Electrochemical behavior of the modified electrode was characterized by differential pulse voltammetry (DPV) and electrochemical impedance spectroscopy (EIS). The AChE concentration and incubation time were optimized at 37.4 °C to achieve the best detection effect. This biosensor exhibits excellent electrochemical properties with a wider linear range of 0.1 ~ 1500 ng·mL^{-1}, lower detection limit of 0.019 ~ 0.077 ng·mL^{-1}, better stability and repeatability, which realizes the rapid detection of total amount of OPPs, and can simultaneously detect a large class of OPPs rather than one kind of OPP. Two OPPs (trichlorfon, dichlorvos) were detected in actual samples of apple and cabbage and achieved satisfactory test results.

1. Introduction

Organophosphorus pesticides (OPPs) are a kind of (thio) phosphate compounds (Shahdost-fard, Fahimi-Kashani, & Hormozi-nezhad, 2021; Wang, Duan, Fan, Zhang, & Zhang, 2021), which are widely used in agricultural production, mainly used as pesticides, a few used as herbicides, fungicides as well as plant growth regulators, and plays a positive role in controlling agricultural diseases and improving the quality and yield of agricultural products (Chen, Chen, Zhao, Liu, & Chi, 2020; Chen, Jin et al., 2020; Mena, González-Ortegón, Solano, & Araújo, 2020; Sharma, Wangoo, & Sharma, 2021). However, the problem of OPPs residues is becoming more and more serious due to the long-term abuse of OPPs, and not only pollute ecological environment, but also harm to human health and life safety (Galaço, Jesus, Freire, de Oliveira, & Serra, 2020; Liu, Li et al., 2020; Liu, Luo et al., 2020; Wang et al., 2020). OPPs are easy to combine with the active center of AChE, which make AChE lose activity and the ability to hydrolyze acetylcholine, so that acetylcholine accumulates in human body, causing disorder of nerve conduction function and a series of poisoning symptoms (Buzyurova et al., 2020; Nazar et al., 2020). A large amount of OPPs intake will cause a series of neurotoxic symptoms, such as respiratory paralysis, and even death in serious cases (Cha et al., 2020; Ma et al., 2020). Long term exposure to or ingestion of low-dose OPPs may cause organ damage, teratogenesis, carcinogenesis and mutation (Lumsden et al., 2020; Savall et al., 2020).

With the change of environmental conditions, there are serious gene mutations in agricultural and forestry insects, and the single OPP has been unable to achieve satisfactory insecticidal effect (Boaventura, Martin, Pozzebon, Mota-Sanchez, & Nauen, 2020; Machamer et al., 2020). Therefore, the use of multiple OPPs mixed in a certain proportion increase gradually. The current national detection standards only make clear provisions for a single limit of OPPs, but not for the total amount of OPPs (Bondoc, 2016a, 2016b, 2016c, 2016d; Monteiro, Witt, Guiloski, dos Santos, & de Assis, 2020; Naime et al., 2020; Urióstegui-Acosta et al., 2020). In order to monitor the content of OPPs in agricultural products in time, monitor the rational use of OPPs, and prevent the excessive OPPs food entering market, it is urgent to research and develop methods and technologies for rapid detection of OPPs residues

* Corresponding authors.
E-mail addresses: zhaoguozheng@sxnu.edu.cn (G. Zhao), zhaobo@njnu.edu.cn (B. Zhao).

https://doi.org/10.1016/j.foodchem.2021.129511
Received 28 November 2020; Received in revised form 31 January 2021; Accepted 28 February 2021
Available online 9 March 2021

and the total amount of OPPs on site.

At present, the detection methods of OPPs mainly include chromatography (Singh, Thakur, Singh, & Kaur, 2020; Zhang, Cao, Zhang, & Yin, 2020; Zhong et al., 2020), enzyme inhibition (Qin et al., 2020; Singh, Balayan, Hooda, Sarin, & Chauhan, 2020; Yang et al., 2019) and immunoassay (Kumar, Vaid, Bansal, & Kim, 2020; Sun, Xiong, Tang, Zeng, & Tang, 2020; Zhang et al., 2020). Chromatography is difficult to meet the requirements of rapid and efficient detection of various departments due to the shortcomings of large-scale instruments, complex instrument operation, professional operation, complex sample pretreatment, long detection cycle and high cost. The enzyme inhibition method has the advantages of short reaction time and simple operation, but the enzyme reagent is easy to be inactivated with unstable results and poor repeatability. Enzyme linked immune sorbent assay (ELISA) is fast, sensitive and does not need expensive equipment, which makes it easy to implement and more suitable for the detection of large quantities of samples on site (Chen, Chen et al., 2020; Chen, Jin et al., 2020; Liu et al., 2020). Among them, indirect competition method is the simplest and most widely used method in ELISA.

Yang *et al.* prepared AChE sensor with patterned structure for detecting dichlorvos based on titanium dioxide sol–gel carrier with the limit of detection of 0.23 nM (Hu, Wang, Li, Wang, & Yang, 2020). A fluorescence visualization paper-based sensor was developed by She *et al.* to detect three OPPs with high stability (Wang et al., 2019). Zhao *et al.* detected six β-agonists by indirect competitive immunoassay with a wide linear range, low detection limit (Gu et al., 2020). So far, only one or a few kinds of OPPs were detected in domestic and foreign research, and there is no detection of total amount of OPPs. In this work, according to indirect competitive method, a new nanogold/mercaptomethamidophos multi-residue electrochemical biosensor was constructed by the combination of nanotechnology, surface chemical modification and biosensor technology to detect simultaneously 11 kinds of OPPs and the total amount of OPPs, and applied to the detection of OPPs in actual samples of apple and cabbage.

2. Experimental section

2.1. Reagents

Dimethoate, parathion, diazinon, omethoate, methomyl, pirimiphos methyl, trichlorfon, fenthion, graphite, chitosan, mercaptoacetic acid, carbodiimide hydrochloride (EDC) and *N*-hydroxysuccinimide (NHS) were purchased from Shanghai Aladdin Biochemical Technology Co., Ltd. Chlorpyrifos, dichlorvos, methamidophos and phoxim were obtained from national standard material network (www.bzwz.com). Bovine serum albumin (BSA), potassium ferricyanide, disodium hydrogen phosphate and sodium dihydrogen phosphate were purchased from Sinopharm Chemical Reagent Co., Ltd. AChE and apple/cabbage were bought from Shanghai Enzyme linked Biotechnology Co., Ltd and Suguo Supermarket, respectively.

2.2. Instruments

Electrochemical performance of constructed biosensor was monitored by a CHI600E electrochemical workstation (Shanghai Chenhua Apparatus Co., Ltd, China). The experiments were performed using a three-electrode system with platinum (Pt) wire, Ag/AgCl, and glassy carbon as counter electrode, reference electrode, and working electrode, respectively. Infrared spectra were measured by a Nicolet IS5 spectrometer (Thermo Fisher Scientific Co., Ltd, USA). The molecular structure was analyzed by AVANCE 400 nuclear magnetic resonance spectrometer (Bruker Corporation, Switzerland).

2.3. Synthesis of mercaptomethamidophos

In order to immobilize methamidophos on gold nanoparticles by Au–S chemical bonds, mercaptomethamidophos containing thiol group was synthesized by amidation of methamidophos. The synthetic route is as follows: 0.1 g methamidophos was dissolved in 10 mL 0.1 $mol{\cdot}L^{-1}$ hydrochloric acid, stirred for 1 h under ice bath conditions, and used as solution A. 254 g EDC and 0.434 g mercaptoacetic acid were dissolved in PBS solution (pH = 7.4) to obtain solution B. Add 0.542 g NHS into solution B and stir at room temperature for 24 h to obtain solution C. Add solution A to solution C slowly and stir for 24 h. The synthesized white solid was evaporated to obtain mercaptomethamidophos and stored at low temperature. The synthesis path is shown in Fig. 1S.

2.4. Preparation of nanogold/mercaptomethamidophos multi-residue electrochemical biosensor

In 1% chloroauric acid solution, a layer of nanogold was plated on the treated glassy carbon electrode (GCE) by electrochemical precipitation method with a potential of −0.2 V and a constant potential of 60 s. 10 μL 0.1 M mercaptomethamidophos was applied on the electrode and dried at 37.5 °C. The electrode was incubated in 1% mercaptohexanol solution for 30 min to block the active sites on the surface of gold nanoparticles which were not bound by mercaptomethamidophos. Finally, the nanogold/mercaptomethamidophos multi-residue electrochemical biosensor was prepared by washing the electrode with PBS solution.

2.5. Characterization

Electrochemical behavior of GCE at different stages was characterized by differential pulse voltammetry (DPV) and electrochemical impedance spectroscopy (EIS), including GCE, GCE/nanogold, GCE/nanogold/mercaptomethamidophos, GCE/nanogold/mercaptomethamidophos/mercaptohexanol, GCE/nanogold/mercaptomethamidophos/mercaptohexanol/AChE. DPV spectrum was determined with voltage range of −0.2 ~ 0.5 V and pulse amplitude of 50 mV in PBS buffer solution (0.1 M, pH 7.4) of 2 mM $K_3[Fe(CN)_6]/K_4[Fe(CN)_6]$. EIS curve was measured with low frequency of 0.01 Hz, high frequency of 10^6 Hz and pulse amplitude of 0.005 V in 0.1 M KCl and 5 mM $K_3[Fe(CN)_6]$ solution.

2.6. Optimization of condition

In order to detect OPPs by nanogold/mercaptomethamidophos multi-residue electrochemical biosensor under optimal conditions, the AChE concentration and incubation time were optimized at 37.4 °C.

Optimization of AChE concentration in incubation solution: PBS incubation solutions with different concentrations of AChE were prepared and applied to the nanogold/mercaptomethamidophos electrochemical biosensor. After incubation at 37.4 °C for 30 min, the electrode surface was washed with PBS, and the peak current value of DPV was measured on the electrochemical workstation.

Optimization of incubation time: The mixed incubation solution of 10 μL AChE (optimal concentration of AChE) and PBS was applied to the nanogold/mercaptomethamidophos electrochemical biosensor. DPV peak current value was measured once every 5 min.

2.7. Detection of OPPs

Under the optimal AChE concentration and incubation time, a series of 10 μL (the ratio of AChE to PBS is 8:2) of different concentrations of OPPs and AChE were prepared and dripped onto nanogold/mercaptomethamidophos electrochemical biosensor, which was incubated at 37.4 °C, washed with PBS buffer solution and placed in PBS buffer solution of 2 mM $K_3[Fe(CN)_6]$. By measuring the change of DPV, the concentration of OPPs was quantitatively detected.

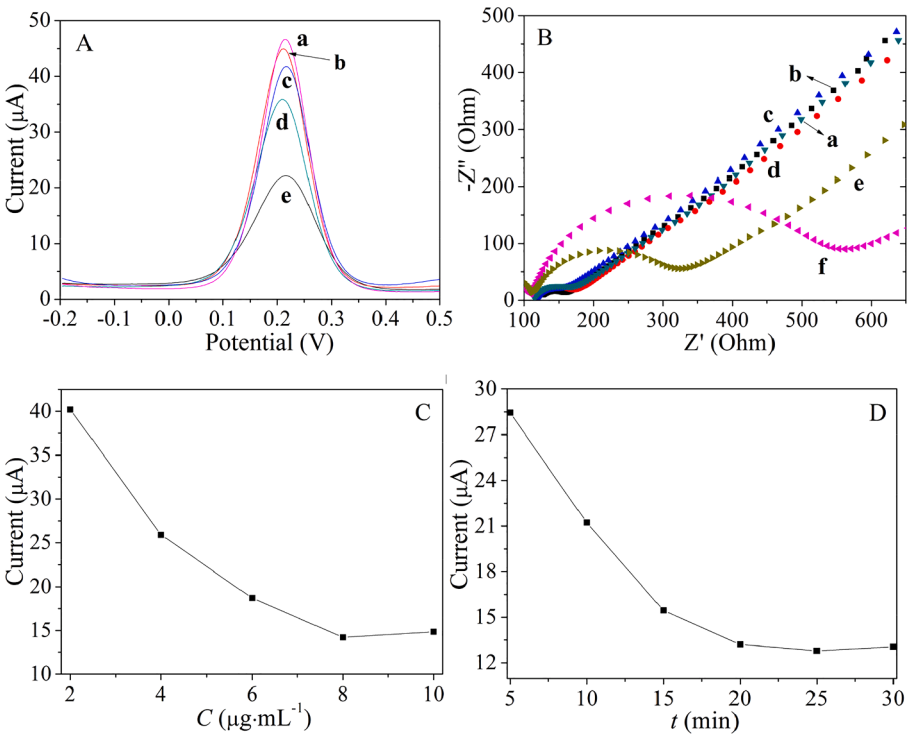

Fig. 1. (A) DPV curves of different stages of electrode modification: (a) GCE/nanogold; (b) GCE; (c) GCE/nanogold/mercaptomethamidophos; (d) GCE/nanogold/mercaptomethamidophos/mercaptohexanol; (e) GCE/nanogold/mercaptomethamidophos/mercaptohexanol/AChE. (B) EIS of electrode modification process: (a) GCE; (b) GCE/nanogold; (c) GCE/nanogold/mercaptomethamidophos; (d) GCE/nanogold/mercaptomethamidophos/mercaptohexanol; (e) GCE/nanogold/mercaptomethamidophos/mercaptohexanol/AChE/dichlorvos; (f) GCE/nanogold/mercaptomethamidophos/mercaptohexanol/AChE. Condition optimization: (C) AChE concentration; (D) incubation time.

2.8. Pretreatment of actual samples

Three clean apple or cabbage samples were chosen, and cut them into pieces about 1 cm^2 (50 ± 0.005 g each). Quantitative addition of trichlorfon/dichlorvos standard solution, adding a certain amount of extraction solution for extraction, transfer into the flask, concentrate to about 2 mL, and dry with nitrogen. 10 mL ethanol solution (volume ratio 1:1) was added and stored in dark at low temperature.

3. Results and discussion

3.1. Detection principle of nanogold/mercaptomethamidophos multi-residue electrochemical biosensor

The detection principle of nanogold/mercaptomethamidophos electrochemical biosensor is shown in Scheme 1. The incubation solution containing OPPs and AChE was coated on nanogold/mercaptomethamidophos electrochemical biosensor. The OPPs in incubation solution competed with methamidophos molecules on nanogold/mercaptomethamidophos electrochemical biosensor to combine AChE in incubation solution. AChE, which is not bound with OPPs in incubation solution, forms phosphorylated acetylcholinesterase with methamidophos on sensor, which hinders the transmission of electrons on electrode surface, thus causing the change of DPV current value. At the same time, the binding amount of AChE and methamidophos on sensor is inversely proportional to that of OPPs in incubation solution. Therefore, there is a good linear relationship between the difference of DPV peak current value ($\Delta I = I_x - I_0$, I_x is the peak current value corresponding to different concentrations of OPPs, I_0 is the peak current value corresponding to the blank sample) and the OPPs content in a certain range of concentration.

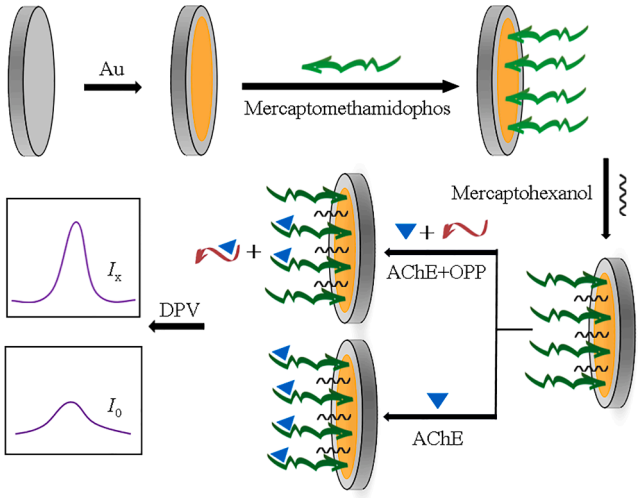

Scheme 1. Detection illustration of nanogold/mercaptomethamidophos electrochemical biosensor.

3.2. Characterization of mercaptomethamidophos

Fig. 3S provides the infrared spectra of mercaptomethamidophos and methamidophos. From Fig. 3S, the modes in 3300 ~ 3500 cm^{-1} are associated with $-NH_2$ characteristic absorption peak of methamidophos. The remarkable signal centering in 3250 cm^{-1} is characterized to the stretching vibration between amide bonds associated with hydrogen bonds. Band at 2880 cm^{-1} and 2750 cm^{-1} is composed of methyl in phosphoester bonds. The strong characteristic peaks at 1670 cm^{-1}, 1570 cm^{-1}, and 1235 cm^{-1} are associated with stretching vibration of carbonyl bonds, bending vibration of N–H bonds, and bending vibration of C–N bonds in amide bonds, respectively. This results showed that mercaptomethamidophos was successfully synthesized.

3.3. Electrochemical characterization of biosensor

Differential pulse voltammetry was used to scan the signal of electrodes in each stage, and the detection results were shown in Fig. 1A. As shown in Fig. 1A, the peak current of bare GCE is about 44 μA (curve b). When GCE was plated by nanogold, the electron transfer on electrode

surface was enhanced due to the strong conductivity of gold nanoparticles. At the same time, the peak current slightly increases to 47.8 μA (curve a) because the gold nanoparticles on electrode hinder electron transfer. When mercaptomethamidophos was modified on the electrode, the peak current decreased slightly to 42.4 μA (curve c), indicating that the modified electrode had little effect on the properties of the electrode. When mercaptohexanol blocked the active sites, the current value decreased to 35.7 μA (curve d). This may be due to the fact that there are active sites on bare nanogold, which mercaptomethamidophos can not occupy, and mercaptohexanol combines with the remaining active sites. After electrochemical reaction with AChE, the peak current decreased to 22 μA (curve e). This is due to the formation of phosphorylated acetylcholinesterase between methamidophos and AChE, which results in the obvious obstruction of electron transfer on electrode surface and the decrease of current value.

The characterization results of EIS are displayed in Fig. 1B. According to Fig. 1B, the electron transfer resistance (R_{et}) of bare GCE and GCE/nanogold are 45 Ω (curve a) and 33 Ω (curve b), respectively, which shows that the electron transfer on electrode surface is enhanced after the gold nanoparticles are modified, at the same time, the modification of gold nanoparticles hinders the electron transfer and the current value changes little. This is consistent with the results of DPV analysis. When mercaptomethamidophos was modified to the electrode, R_{et} increased to 37 Ω (curve c), indicating that the effect of mercaptomethamidophos on the biosensor was slight. When mercaptohexanol blocked the active site, R_{et} increased slightly to 51 Ω (curve d), due to the influence of mercaptohexanol binding with nanogold on electron transfer. After electrochemical reaction with AChE, R_{et} increased rapidly to 213 Ω (curve e), suggesting that AChE binds with methamidophos on electrode surface to form phosphorylated acetylcholinesterase, which hinders the electron transfer. Finally, R_{et} increased to 449 Ω when only AChE was added, which indicated that the current value was related to the content of AChE.

3.4. Optimization of condition

The optimized results of AChE concentration and incubation time are shown in Fig. 1C and D. From Fig. 1C and D, the current value decreased with the increase of AChE concentration. When the concentration of AChE is 8 μg·mL^{-1}, the current value reaches minimum, and when the concentration exceeds 8 μg·mL^{-1}, the current value increases slightly, which indicates that AChE is saturated at this time. Therefore, the optimal concentration of AChE is 8 μg·mL^{-1}. In the competitive reaction between OPPs, methamidophos and AChE, the binding amount of AChE and methamidophos increased with increasing incubation time. The current value decreased rapidly with the increase of incubation time. After 25 min, the current value remained unchanged, then slightly increased, indicating that AChE is saturated, so 25 min was the best time.

3.5. DPV detection of OPPs

11 kinds of OPPs, including chlorpyrifos, dichlorvos, methamidophos, dimethoate, parathion, phoxim, omethoate, trichlorfon, pirimiphos methyl, diazinon, fenthion and one carbamate (the standard solution of methomyl) were detected by nanogold/mercaptomethamidophos multi-residue electrochemical biosensor. DPV was used to scan the electrical signals of OPPs with different concentrations, and the superposition curves were plotted in Fig. 2. As demonstrated in Fig. 2, after the electrochemical biosensor was incubated in incubation solution containing OPPs/methomyl and AChE, the peak current value of DPV gradually decreased. This is because OPPs or methomyl in solution and AChE form phosphorylated acetylcholinesterase or carbamyl acetylcholinesterase, which inhibites the transmission of electrons on electrode. The more phosphorylated acetylcholinesterase or carbamyl acetylcholinesterase is formed, the more obvious the blocking effect, the lower the peak current value of DPV. At the same concentration, the electrochemical response for OPPs or methomyl detection was in a sequence of phoxim > chlorpyrifos > fenthion > dimethoate > omethoate > parathion > diazinon > dichlorvos > methomyl > trichlorfon > methamidophos > pirimiphos methyl. The higher the concentration of OPPs or methomyl, the greater the peak current value; the larger the difference of concentration, the greater the difference of peak current value, indicating that the difference of DPV peak current value ΔI is directly proportional to the content of OPPs or methomyl in solution.

Comparison of detection results of 11 OPPs and methomyl are represented in Table 1. From Table 1, the slope of linear relationship of OPPs was close (about 0.02), and the relative standard deviation was 5.044%. The slope of linear relationship of methomyl is slightly higher than those of OPPs. This is because the formation mechanisms of OPPs and AChE are the same, they both produce phosphorylated acetylcholinesterase, while methomyl belongs to carbamate, which produces carbamyl acetylcholinesterase. The structures of two enzymes are different, and the obstruction to electron transfer is also different. The linear range, detection limit and correlation coefficient for OPPs are 0.1 ~ 1500 ng·mL^{-1}, 0.019 ~ 0.077 ng·mL^{-1} and 0.9905 ~ 0.9992, respectively, proving that nanogold/mercaptomethamidophos multi-residue electrochemical biosensor manifests excellent properties with a wide linear range and low detection limit, which is attributed to the high specific surface area of GCE/nanogold/mercaptomethamidophos caused by nanoscale effect and good conductivity of gold nanoparticles, increasing loading capacity of OPPs. Furthermore, it is helpful to the immobilization of mercaptomethamidophos on electrode surface through Au–S bonds. This ensures that AChE can be adhered to the electrode surface in a large amount due to the strong interaction between AChE and mercaptomethamidophos.

3.6. Detection of total OPPs, stability and repeatability

Four kinds of commonly used OPPs were mixed in different proportions to prepare mixed solutions of different concentrations. The results are shown in Table 1S and Table 2S. The relative deviation of nanogold/mercaptomethamidophos multi-residue electrochemical biosensor is within 5% when the detection range of total OPPs is 950 ng·mL^{-1} ~ 50 ng·mL^{-1}, which is suitable for pesticide detection. The electrochemical biosensors were placed at 37.4 °C for 1 day, 2 days, 3 days, 4 days, 5 days, 6 days, 7 days, 8 days, 9 days and 10 days, respectively. It was found that the standard deviation of the slope of the linear relationship was 3.8% in the detection results of methamidophos with 10 electrodes, which indicated that the stability was fine for nanogold/mercaptomethamidophos electrochemical biosensor. In order to verify the repeatability of nanogold/mercaptomethamidophos electrochemical biosensor, seven different electrodes were selected to detect methamidophos with three different concentrations. The standard deviation of the measured values was between 5.5% and 8.6%, which shows that nanogold/mercaptomethamidophos electrochemical biosensor can be reused, and greatly increases practical use ability of the biosensor.

3.7. Detection of actual samples

In order to evaluate the detection performance of nanogold/mercaptomethamidophos multi-residue electrochemical biosensor in practical system, two OPPs (trichlorfon, dichlorvos) with high toxicity were selected as detection objects with low, medium and high concentrations in standard addition recovery experiments. The test results are described in Tables 2 and 3. From Tables 2 and 3, the average recovery was 81.45%~116.81%, and the relative standard deviation was within 10%, meeting the requirements of recovery standard, which indicates that nanogold/mercaptomethamidophos electrochemical biosensor can effectively detect OPPs.

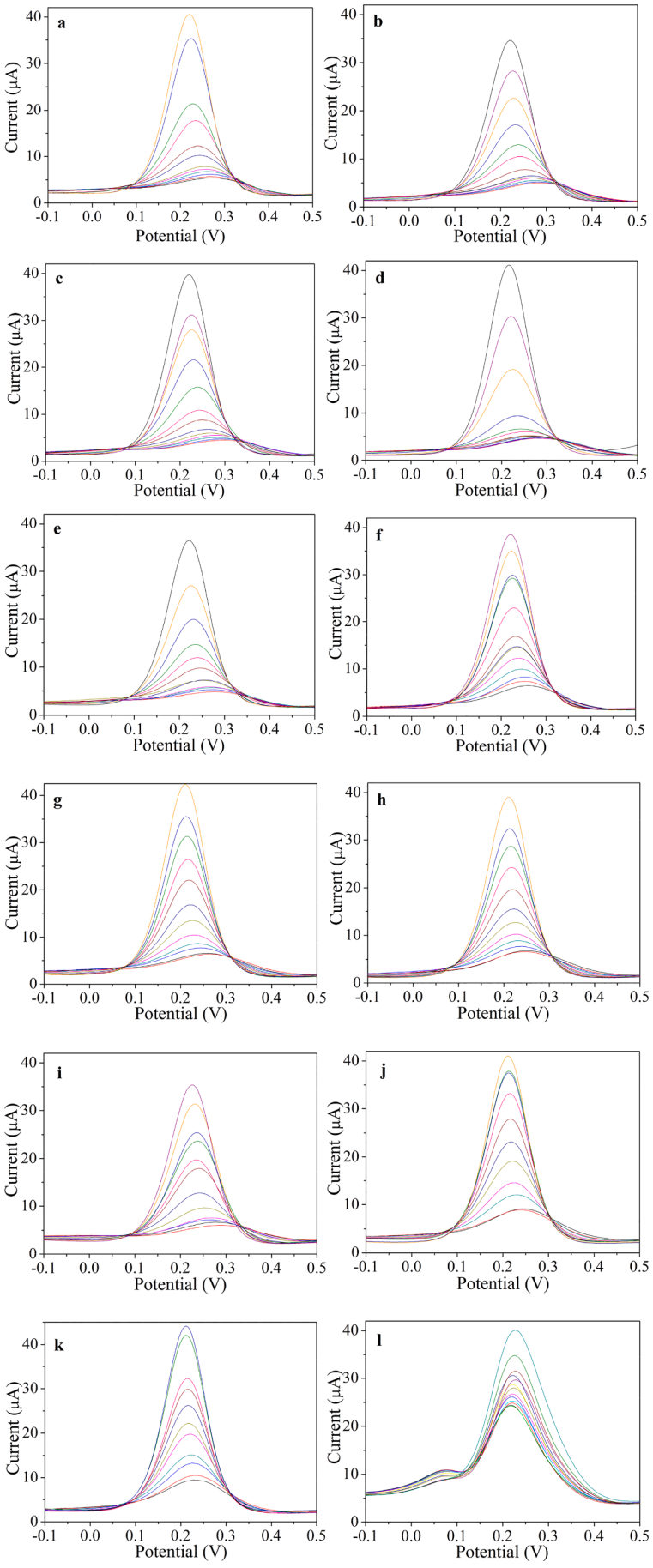
a
b
c
d
e
f
g
h
i
j
k
l
Current (μA)
Potential (V)

Fig. 2. DPV of (a) omethoate, (b) pirimiphos methyl, (c) diazinon, (d) fenthion, (e) trichlorfon, (f) methomyl, (g) chlorpyrifos, (h) dichlorvos, (i) methamidophos, (j) dimethoate, (k) phoxim, and (l) parathion detection by nanogold/mercaptomethamidophos multi-residue electrochemical biosensor: the concentrations from top to bottom were 1500 ng·mL^{-1}, 1200 ng·mL^{-1}, 800 ng·mL^{-1}, 600 ng·mL^{-1}, 400 ng·mL^{-1}, 200 ng·mL^{-1}, 100 ng·mL^{-1}, 50 ng·mL^{-1}, 10 ng·mL^{-1}, 1 ng·mL^{-1} and 0 ng·mL^{-1}.

Table 1
Comparison of detection results of 11 OPPs and methomyl.

Detection object	Linear relationship	Correlation coefficient	Linear range (ng·mL^{-1})	Detection limit (ng·mL^{-1})
Parathion	Y = 0.02088X + 17.1950	0.9905	0.1 ~ 1500	0.034
Chlorpyrifos	Y = 0.02392X + 5.2355	0.9992		0.056
Dichlorvos	Y = 0.02151X + 5.5914	0.9992		0.022
Methamidophos	Y = 0.01981X + 4.4055	0.9912		0.031
Dimethoate	Y = 0.02484X + 9.9014	0.9961		0.019
Phoxim	Y = 0.02212X + 10.3138	0.9968		0.041
Omethoate	Y = 0.02248X + 3.7968	0.9925		0.030
Pirimiphos methyl	Y = 0.02030X + 3.3234	0.9965		0.077
Diazinon	Y = 0.02390X + 3.1964	0.9939		0.055
Fenthion	Y = 0.02565X + 1.6715	0.9926		0.043
Trichlorfon	Y = 0.02163X + 3.4394	0.9937		0.021
Methomyl	Y = 0.03817X + 6.1317	0.9917		0.081

Table 2
Detection of dichlorvos in apple samples.

Amount added (ng·mL^{-1})	Actual concentration (ng·mL^{-1})	Recovery (%)	Average recovery (%)	RSD (%)
100	90.65	90.65	86.00	6.37
	87.40	87.40		
	79.96	79.96		
400	400.2	100.05	111.88	9.20
	475.1	118.78		
	467.2	116.80		
1000	838.2	83.82	84.04	3.21
	868.4	86.84		
	814.5	81.45		

4. Conclusions

In this paper, the mercaptomethamidophos was successfully prepared as a substrate. Using indirect competitive method, the simultaneous rapid detection of 11 kinds of OPPs and total amount of OPPs with high sensitivity was achieved by nanogold/mercaptomethamidophos multi-residue electrochemical biosensor with the combination of nanoscale effect, strong Au–S bonds and interaction between AChE and mercaptomethamidophos. In the process of incubation, the optimal AChE concentration and incubation time are 8 μg·mL^{-1} and 25 min, respectively. The lower OPPs concentration, the smaller peak current value; the larger the difference of OPPs concentration, the greater the difference of peak current value, which the reason is that OPPs and AChE form phosphorylated acetylcholinesterase in solution, blocking the transmission of electrons on electrode surface. The nanogold/mercaptomethamidophos multi-residue electrochemical biosensor indicates superior properties with a wide linear range (0.1 ~ 1500 ng·mL^{-1}), low detection limit (0.019 ~ 0.077 ng·mL^{-1}), and good correlation coefficient (0.9905 ~ 0.9992), which can be ascribed to the innovative design strategy. This biosensor has good stability and repeatability, realizing the rapid detection of total amount of OPPs, and can simultaneously detect a large class of OPPs rather than one kind of OPP. The average recovery and relative standard deviation of trichlorfon and dichlorvos detection in the actual samples of apple and cabbage were performed, which shows great potential for the applications in environmental and food safety detection.

Table 3
Detection of trichlorfon in cabbage samples.

Amount added (ng·mL^{-1})	Actual concentration (ng·mL^{-1})	Recovery (%)	Average recovery (%)	RSD (%)
100	113.90	113.90	103.82	8.63
	96.69	96.69		
	100.88	100.88		
400	439.30	123.33	116.81	6.52
	433.75	108.44		
	474.66	118.67		
1000	822.87	82.29	81.45	1.80
	822.87	82.29		
	797.76	79.78		

CRediT authorship contribution statement

Guozheng Zhao: Writing - original draft, Methodology, Investigation. **Binhua Zhou:** Visualization, Investigation. **Xiuwen Wang:** Data curation, Validation. **Jian Shen:** Methodology, Conceptualization. **Bo Zhao:** Project administration, Supervision.

Declaration of Competing Interest

The authors declare that they have no known competing financial interests or personal relationships that could have appeared to influence the work reported in this paper.

Acknowledgements

This work was supported by Transformation of Scientific and Technological Achievements Programs of Higher Education Institutions in Shanxi (No. 2020CG032), National Key Research and Development Project (No. 2020YFF0218300), Linfen Key Research and Development Projects (Social Development) (No. 1909), Cultivation Plan of Young

Scientific Researchers in Higher Education Institutions of Shanxi Province, Scientific and Technological Innovation Programs of Higher Education Institutions in Shanxi (No. 2019L0469), and the Fund for Shanxi "1331 Project". We were indebted to Jiangsu Chemical Reagent Engineering Technology Research Center of Nanjing Chemical Reagent Co., Ltd for many helpful support of our work.

Appendix A. Supplementary data

Supplementary data to this article can be found online at https://doi.org/10.1016/j.foodchem.2021.129511.

References

Boaventura, D., Martin, M., Pozzebon, A., Mota-Sanchez, D., & Nauen, R. (2020). Monitoring of target-site mutations conferring insecticide resistance in spodoptera frugiperda. *Insects, 11*(8), 545.

Bondoc, I. (2016). European regulation in the veterinary sanitary and food safety area, a component of the European policies on the safety of food products and the protection of consumer interests: A 2007 retrospective. Part one: the role of European institutions in laying down and passing laws specific to the veterinary sanitary and food safety area. Revista Universul Juridic, 12-15.

European regulation in the veterinary sanitary and food safety area, a component of the European policies on the safety of food products and the protection of consumer interests: A 2007 retrospective. Part two: regulations. Revista Universul Juridic, 16-19.

European regulation in the veterinary sanitary and food safety area, a component of the European policies on the safety of food products and the protection of consumer interests: A 2007 retrospective. Part three: directives. Revista Universul Juridic, 20-23.

Bondoc, I. (2016). European regulation in the veterinary sanitary and food safety area, a component of the European policies on the safety of food products and the protection of consumer interests: A 2007 retrospective. Part four: decisions. Revista Universul Juridic, 24-27.

Buzyurova, D. N., Pashirova, T. N., Zueva, I. V., Burilova, E. A., Shaihutdinova, Z. M., Rizvanova, I. K., … Souto, E. B. (2020). Surface modification of pralidoxime chloride-loaded solid lipid nanoparticles for enhanced brain reactivation of organophosphorus-inhibited AChE: Pharmacokinetics in rat. *Toxicology, 444*, Article 152578.

Cha, B. S., Lee, E. S., Kim, S., Kim, J. M., Hwang, S. H., Oh, S. S., & Park, K. S. (2020). Simple colorimetric detection of organophosphorus pesticides using naturally occurring extracellular vesicles. *Microchemical Journal, 158*, Article 105130.

Chen, J. L., Chen, X. J., Zhao, J., Liu, S. W., & Chi, Z. G. (2020). Instrument-free and visual detection of organophosphorus pesticide using a smartphone by coupling aggregation-induced emission nanoparticle and two-dimension MnO2 nanoflake. *Biosensors & bioelectronics, 170*, 112668–112676.

Chen, G., Jin, M. J., Ma, J., Yan, M. M., Cui, X. Y., Wang, Y. S., … Wang, J. (2020). Competitive bio-barcode immunoassay for highly sensitive detection of parathion based on bimetallic nanozyme catalysis. *Journal of Agricultural and Food Chemistry, 68*(2), 660–668.

Galaço, A. R. B. S., Jesus, L. T., Freire, R. O., de Oliveira, M., & Serra, O. A. (2020). Experimental and theoretical studies of glyphosate detection in water by an europium luminescent complex and effective adsorption by HKUST-1 and IRMOF-3. *Journal of Agricultural and Food Chemistry, 68*(36), 9664–9672.

Gu, C. X., Ren, P. F., Zhang, F., Zhao, G. Z., Shen, J., & Zhao, B. (2020). Detection of six beta-agonists by three multiresidue immunosensors based on an anti-bovine serum albumin-ractopamine-clenbuterol-salbutamol antibody. *ACS Omega, 5*(10), 5548–5555.

Hu, H. Y., Wang, B., Li, Y. R., Wang, P. C., & Yang, L. Q. (2020). Acetylcholinesterase sensor with patterned structure for detecting organophosphorus pesticides based on titanium dioxide sol-gel carrier. *Electroanalysis, 32*(8), 1834–1842.

Kumar, V., Vaid, K., Bansal, S. A., & Kim, K.-H. (2020). Nanomaterial-based immunosensors for ultrasensitive detection of pesticides/herbicides: Current status and perspectives. *Biosensors & bioelectronics, 165*, 112382. https://doi.org/10.1016/j.bios.2020.112382.

Liu, B. B., Li, P., Wang, Y. L., Guo, Y. R., Zhang, H. X. Y., Dong, S., … Zhang, C. Z. (2020). Quantum dot submicrobead-based immunochromatographic assay for the determination of parathion in agricultural products. *Food Analytical Methods, 13*(9), 1736–1745.

Liu, Y. E., Luo, X. J., Guan, K. L., Huang, C. C., Zhu, C. Y., Qi, X. M., … Mai, B. X. (2020). Legacy and emerging organophosphorus flame retardants and plasticizers in frogs: Sex difference and parental transfer. *Environmental Pollution, 266*, Article 115336.

Lumsden, E. W., McCowan, L., Pescrille, J. D., Fawcett, W. P., Chen, H. G., Albuquerque, E. X., … Pereira, E. F. R. (2020). Learning and memory retention deficits in prepubertal guinea pigs prenatally exposed to low levels of the organophosphorus insecticide malathion. *Neurotoxicology and Teratology, 81*, Article 106914.

Ma, R. X., Xu, M., Liu, C., Shi, G. Y., Deng, J. J., & Zhou, T. S. (2020). Stimulus response of GQD-sensitized Tb/GMP ICP nanoparticles with dual-responsive ratiometric fluorescence: Toward point-of-use analysis of acetylcholinesterase and organophosphorus pesticide poisoning with acetylcholinesterase as a biomarker. *ACS Applied Materials & Interfaces, 12*(37), 42119–42128.

Machamer, J. B., Apland, J. P., Winner, B. M., Wolfe, S. E., Pagarigan, K. T., Bounader, K. M., … McNutt, P. M. (2020). Functional basis for dose-dependent antagonism of rat and rabbit neuromuscular transmission by the bis-pyridinium oxime MMB4. *Archives of Toxicology, 94*(11), 3877–3891.

Mena, F., González-Ortegón, E., Solano, K., & Araújo, C. V. M. (2020). The effect of the insecticide diazinon on the osmoregulation and the avoidance response of the white leg shrimp (Penaeus vannamei) is salinity dependent. *Ecotoxicology and Environmental Safety, 206*, 111364.

Monteiro, L. B., Witt, L. G., Guiloski, I. C., dos Santos, R. S. S., & de Assis, H. C. S. (2020). Evaluation of resistance management for the oriental fruit moth (Lepidoptera: Tortricidae) to insecticides in Brazilian apple orchards. *Journal of Economic Entomology, 113*(3), 1411–1418.

Naime, A. A., Lopes, M. W., Colle, D., Dafre, A. L., Sunol, C., da Rocha, J. B. T., … Farina, M. (2020). Glutathione in chlorpyrifos-and chlorpyrifos-oxon-induced toxicity: A comparative study focused on non-cholinergic toxicity in HT22 cells. *Neurotoxicity Research, 38*(3), 603–610.

Nazar, M. Z., Freed, S., Hussain, S., Sumra, M. W., Shah, M. S., & Naeem, A. (2020). Characteristics of biochemical resistance mechanism of novel insecticides in phenacoccus solenopsis tinsley (Hemiptera: Pseudococcidae). *Crop Protection, 138*, 105320. https://doi.org/10.1016/j.cropro.2020.105320.

Qin, Y., Wu, Y., Chen, G. J., Jiao, L., Hu, L. Y., Gu, W. L., & Zhu, C. Z. (2020). Dissociable photoelectrode materials boost ultrasensitive photoelectrochemical detection oforganophosphorus pesticides. *Analytica Chimica Acta, 1130*, 100–106.

Savall, A. S. P., Fidelis, E. M., Angonesi, V., Bresolin, L., Gervini, V. C., Quines, C., … Pinton, S. (2020). Antidepressant-like effect of (3Z)-5-chloro-3-(hydroxyimino) indolin-2-one in rats exposed to malathion: Involvement of BDNF-Trk beta pathway and AchE. *Life Sciences, 256*, Article 117892.

Shahdost-fard, F., Fahimi-Kashani, N., & Hormozi-nezhad, M. R. (2021). A ratiometric fluorescence nanoprobe using CdTe QDs for fast detection of carbaryl insecticide in apple. *Talanta, 221*, 121467.

Sharma, D., Wangoo, N., & Sharma, R. K. (2021). Sensing platform for pico-molar level detection of ethyl parathion using Au-Ag nanoclusters based enzymatic strategy. *Talanta, 221*, 121267.

Singh, A. P., Balayan, S., Hooda, V., Sarin, R. K., & Chauhan, N. (2020). Nano-interface driven electrochemical sensor for pesticides detection based on the acetylcholinesterase enzyme inhibition. *International Journal of Biological Macromolecules, 164*, 3943–3952.

Singh, J., Thakur, S., Singh, R., & Kaur, V. (2020). Schiff base - Zn(2+)ion combo as 'pick and degrade' probe for selected organophosphorus chemical weapon mimics and flame retardant analog: Detoxification of fruits and vegetables in aqueous media. *Food Chemistry, 327*, Article 127080.

Sun, Y. F., Xiong, P. Y., Tang, J., Zeng, Z. Y., & Tang, D. P. (2020). Ultrasensitive split-type electrochemical sensing platform for sensitive determination oforganophosphorus pesticides based on MnO2 nanoflower-electron mediator as a signal transduction system. *Analytical and Bioanalytical Chemistry, 412*(25), 6939–6945.

Urióstegui-Acosta, M., Tello-Mora, P., Solís-Heredia, M.d. J., Ortega-Olvera, J. M., Piña-Guzmán, B., Martín-Tapia, D., … Quintanilla-Vega, B. (2020). Methyl parathion causes genetic damage in sperm and disrupts the permeability of the blood-testis barrier by an oxidant mechanism in mice. *Toxicology, 438*, 152463.

Wang, J., Duan, H. L., Fan, L.i., Zhang, J., & Zhang, Z. Q. (2021). A magnetic fluorinated multi-walled carbon nanotubes-based QuEChERS method fororganophosphorus pesticide residues analysis in Lycium ruthenicum Murr. *Food Chemistry, 338*, 127805–127810.

Wang, Y. Y., Maruthamuthu, M. K., Jeong, J., Yoo, I. K., Kim, T. W., & Hong, S. H. (2020). Development of fenitrothion adsorbing recombinant Escherichia coli by cell surface display ofpesticide-binding peptide. *Journal of Biotechnology, 322*, 90–95.

Wang, Q., Yin, Q. B., Fan, Y., Zhang, L., Xu, Y., Hu, O., … She, Y. B. (2019). Double quantum dots-nanoporphyrin fluorescence-visualized paper-based sensors for detectingorganophosphorus pesticides. *Talanta, 199*, 46–53.

Yang, N., Zhou, X., Yu, D. F., Jiao, S. Y., Han, X., Zhang, S. L., … Mao, H. P. (2019). Pesticide residues identification by impedance time-sequence spectrum of enzyme inhibition on multilayer paper-based microfluidic chip. *Journal of Food Process Engineering*. e13544.

Zhang, Q. S., Cao, X. L., Zhang, Z. P., & Yin, J. G. (2020). Preparation of magnetic flower-like molybdenum disulfide hybrid materials for the extraction oforganophosphorus pesticides from environmental water samples. *Journal of Chromatography A, 1631*, Article 461583.

Zhang, C., Jiang, Z. J., Jin, M. J., Du, P. F., Chen, G., Cui, X. Y., … Wang, J. (2020). Fluorescence immunoassay for multiplex detection of organophosphate pesticides in agro-products based on signal amplification of gold nanoparticles and oligonucleotides. *Food Chemistry, 326*, Article 126813.

Zhong, M. Y., Tang, J. H., Guo, X. Y., Guo, C., Li, F., & Wu, H. F. (2020). Occurrence and spatial distribution of organophosphorus flame retardants and plasticizers in the Bohai, Yellow and East China seas. *Science of the Total Environment, 741*, 140434.